Absolute Rate, Evolving Luminosity Function, and Evolving Jet Opening Angle Distribution for Long Gamma-Ray Bursts

Tatsushi Matsubayashi,[1,*)] Ryo Yamazaki,[2,3,**)] Daisuke Yonetoku,[4,***)] Toshio Murakami[4,†)] and Toshikazu Ebisuzaki[1,††)]

[1]*Ebisuzaki Computational Astrophysics laboratory, Institute of Physical and Chemical Research (RIKEN), Wako, 351-0198 Japan*
[2]*Department of Earth and Space Science, Osaka University, Toyonaka 560-0043, Japan*
[3]*Department of Physics, Hiroshima University, Higashi-Hiroshima, 739-8526, Japan*
[4]*Department of Physics, Kanazawa University, Kanazawa, 920-1192, Japan*

(Received April 19, 2005)

Using the luminosity function and the apparent GRB rate inferred from the spectral peak energy-luminosity relation, we investigate the absolute GRB formation rate, taking into account the effects of both the jet-luminosity evolution and the jet opening angle evolution. In the case that there is no jet opening angle evolution, the jet-corrected luminosity for high-redshift GRBs is much larger than typical values for low-z ($z \sim 1$) bursts. On the other hand, if the jet-luminosity does not evolve with time, the jet opening angle for high-z bursts should be much smaller than that for low-z GRBs. Therefore, it is preferable to take into account both evolution effects. We also estimate the local GRB event rate in a galaxy of $\sim 10^{-7}$–10^{-5} yr^{-1}.

§1. Introduction

The luminosity function and the formation rate history of gamma-ray bursts (GRBs) are important for understanding the nature of these events. The formation history of GRBs provides constraints on the population of progenitors. If we know the absolute value of the GRB rate, we can study their relation to other objects potentially related to GRBs. It is fairly certain that long GRBs arise from relativistic jets with typical opening half-angles of ~ 0.1 rad.[25),43)] For this reason, determining the corrections due to jet collimation and/or jet structure is essential in the study of the GRB rate. The luminosity function may directly reflect the properties of the progenitor, such as the jet structure, the jet kinematics, and so on.

GRBs could be useful tools to investigate high redshift objects. The connection between long duration GRBs and supernovae is strongly suggested, and it is known that at least some GRBs arise from the collapse of massive stars.[7),12),38),16)] The universe began to reionize at $z \sim 17$,[37)] which implies that the first generation objects

*) E-mail: tatsushi@riken.jp
**) E-mail: ryo@vega.ess.sci.osaka-u.ac.jp
***) E-mail: yonetoku@astro.s.kanazawa-u.ac.jp
†) E-mail: murakami@astro.s.kanazawa-u.ac.jp
††) E-mail: ebisu@riken.jp

had already been formed by at least $z \sim 20$. Because they are massive, they immediately exploded and produced GRBs at a redshift of $z \sim 20$. Indeed, some of their prompt emissions and afterglows are bright enough to be actually detected.[20),6)] The absolute rate of prompt GRB emissions may provide some information concerning the cosmic star formation history.[39),28)] Also, the afterglows of high-z GRBs may provide information concerning the cosmic reionization history.[18),17),19),11),3)]

Many authors have attempted to derive the luminosity function and absolute rate of GRBs. Schmidt[34)] derived the luminosity function and the absolute value of the local GRB rate so that $\langle V/V_{\rm max}\rangle$ and the observed event rate of BATSE bursts are reproduced. Later, he obtained the $\langle V/V_{\rm max}\rangle$-hardness relation for BATSE GRBs that was used to determine the luminosity function and the absolute local GRB rate.[35)] The value he derived is ~ 0.5 Gpc^{-3}yr^{-1}. However, in that derivation, the geometrical corrections were not considered. The luminosity function and the formation rate history of long GRBs have been simultaneously derived using some luminosity indicators, such as the luminosity-variability relation[8),22)] and the luminosity-lag relation.[29),27)] Recently, it was found that the spectral peak energy is correlated with the peak luminosity with actually known distances of up to $z \sim 4.5$.[41)] The correlation is tightest in such kinds of luminosity indicators.[1),2),13)] Using the peak energy-luminosity relation as a luminosity indicator, Yonetoku et al.[41)] investigated the apparent GRB luminosity function (see § 2.1) and the GRB formation rate for redshifts $z \lesssim 12$ and suggested that the GRB formation rate rapidly increases up to $z \sim 1$ and then continues to increase toward higher redshifts $z \sim 12$. This behavior of the formation history is somewhat similar to those derived using other luminosity indicators.[8),22),27)]

There is evidence suggesting that the (isotropic-equivalent) luminosity evolution of GRBs takes the form $\propto (1+z)^{2.6}$,[41)] which is quite similar to that of quasars.[5),24)] The luminosity evolution for GRBs has been independently reported.[22),40),9),41)] The origin of the luminosity evolution is not yet clear. The jet-corrected luminosity, $L_j = Lf_b$, where $f_b = {\theta_j}^2/2$ is the beaming factor and θ_j is the jet opening half-angle, clusters very near the standard value.[21)] The same is true for the jet-corrected energy.[10),4),13)] These facts suggest that the luminosity evolution may result from either jet-opening angle evolution[22)] or jet-luminosity evolution.

The effect of jet collimation is investigated explicitly in Ref. 14), where the luminosity function is studied assuming that its functional form is a double power-law and that the jet-corrected luminosity L_j is constant. For the structured jet case, general formulae to calculate the luminosity function and/or the local GRB rate from the angular distribution of kinetic energies in the jet has been presented.[31),15)] One crucial assumption in these works is that the apparent GRB rate is proportional to the cosmic star formation rate. Furthermore, in Ref. 14), luminosity evolution is not considered.

In this paper, using the luminosity function and the apparent GRB rate derived in Ref. 41), we study the absolute GRB formation rate, taking into account the effects of both the jet-luminosity evolution and the jet opening angle evolution. A general formula to calculate the true GRB rate is presented. The most important point in the derivation is the geometrical correction of the jet opening angle, θ_j.

Instead of using the distribution function for θ_j, we consider an approach similar to that used in Ref. 14). The fact that the jet-corrected luminosity L_j clusters in narrow ranges[21] enables us to calculate the jet-correction factors without directly taking into account the opening angle distribution. We also study the opening angle evolution. If we assume that the origin of the luminosity evolution is the jet opening angle evolution, the high-redshift GRBs are collimated much more tightly than the nearby events. Throughout the paper, we assume a flat, isotropic universe with $\Omega_M = 0.32, \Omega_\Lambda = 0.68$, and $h = 0.72$.

§2. The absolute GRB formation rate

2.1. *Apparent luminosity function of GRBs*

The apparent luminosity function of GRBs, that is the rate of actually detected GRBs per unit comoving volume at a redshift z and a peak luminosity L, is written

$$\Phi(L, z) = \rho(z)\phi(L/g(z))/g(z) \quad , \tag{2·1}$$

where $\rho(z)$, $g(z)$, and $\phi(L')$ are the GRB formation rate, the luminosity evolution, and the local luminosity function, respectively.[5),24),22)] In this paper, we adopt the functional forms of these quantities given below, as derived in Ref. 41).

The GRB formation rate is given by

$$\rho(z) = \rho_0 \begin{cases} [(1+z)/2]^{6.0} & 0 < z < 1 \quad , \\ [(1+z)/2]^{0.4} & 1 < z < z_{\max} \quad , \\ 0 & z_{\max} < z \quad , \end{cases} \tag{2·2}$$

where $\rho_0 = \rho(z = 1)$ is the normalization constant, and $z_{\max}$ is the epoch at which the first GRBs formed. Here we assume a broken power-law form. However, the results obtained in the present paper are almost unchanged if other smooth functions are adopted.

The luminosity evolution is assumed to take the form

$$g(z) = \left(\frac{1+z}{2}\right)^{\alpha} \quad , \tag{2·3}$$

where, throughout the paper, we adopt $\alpha = 2.6$, as derived in Ref. 41).

The local luminosity function $\phi(L')$, where $L' \equiv L/g(z)$ represents the peak luminosity after removing the luminosity evolution effect, is derived from the universal cumulative luminosity function $\psi(L')$ as

$$\phi(L') = -\frac{d}{dL'}\psi(L') \quad , \tag{2·4}$$

and we assume the following form of $\psi(L')$ in the range $L'_{\min} < L' < L'_{\max}$:

$$\psi(L') = \psi_0 \left(L'/L'_*\right)^A \left[1 + \left(L'/L'_*\right)^s\right]^{(B-A)/s} \quad . \tag{2·5}$$

Here A and B are the power law indices in the asymptotic forms, and s describes the smoothness of the transitions between the high and low L' regimes. We set

these parameters as $A = -0.29$, $B = -1.02$, and $s = 2.6$, in order to reproduce the results presented in Fig. 6 of Ref. 41). Therefore, the break point of $\psi(L')$ is $L'_* = 1.1 \times 2^\alpha \times 10^{51}$ erg s^{-1}, because the functional form of $g(z)$ adopted in this paper has an extra factor of 2^α compared with that used in Ref. 41). Finally, the normalization constant ψ_0 is chosen so as to satisfy

$$\int_{L'_{\rm min}}^{L'_{\rm max}} \phi(L')dL' = 1 \quad . \tag{2·6}$$

As suggested in Ref. 41), we assume the universality of the local luminosity function $\phi(L')$. Then, both $L'_{\rm max}$ and $L'_{\rm min}$ should be independent of z; that is, we can write

$$\begin{cases} L_{\rm max}(z) = L'_{\rm max} \times g(z) \quad , \\ L_{\rm min}(z) = L'_{\rm min} \times g(z) \quad . \end{cases} \tag{2·7}$$

Hence both the maximum and the minimum values of the luminosity evolve with $g(z)$. In the fiducial case, the values $L'_{\rm max} = 1 \times 10^{54}$ erg s^{-1} and $L'_{\rm min} = 1 \times 10^{49}$ erg s^{-1} are adopted.[41)]

We determine the normalization constant ρ_0 as follows. The actual event rate of BATSE-observed bursts, with observed peak fluxes larger than $F_{\rm obs}$, is given by

$$N_{\rm obs}(> F_{\rm obs}) = \zeta_{\rm exp} \int_0^{z_{\rm lim}} dz \, \frac{1}{1+z} \frac{dV}{dz} \int_{L_{\rm lim}(z)}^{L_{\rm max}(z)} dL \, \Phi(L, z) \quad , \tag{2·8}$$

where V, $L_{\rm lim}$, and $z_{\rm lim}$ are the comoving volume, the limiting flux for given z, and the upper bound on the redshift, respectively. The mean exposure efficiency $\zeta_{\rm exp}$ is approximately 48% for the BATSE experiment.[30)] The limiting flux can be written as

$$L_{\rm lim}(z) = 4\pi d_L(z)^2 \times F_{\rm obs}, \tag{2·9}$$

where $d_L(z)$ is the luminosity distance. In Ref. 41), 689 BATSE bursts were considered. Their observed peak fluxes in the 30–10000 keV band are larger than 2×10^{-7} erg cm^{-2}s^{-1} and their redshifts are smaller than $12 (= z_{\rm lim})$. The corresponding observation period is 9.0 yrs, because they selected the GRB sources from ID# 105(1991.111) to ID# 8121(2000.147) (see Table 2 of Ref. 41)). Hence we find $N_{\rm obs}(> 2 \times 10^{-7}$ erg cm^{-2}s$^{-1}) \sim 76.6$ events yr^{-1}. We can determine the value of the normalization constant ρ_0 needed to reproduce this value. The results are shown in Table I. It is found that ρ_0 changes by a few percent if $L'_{\rm max}$ ranges between 1×10^{53} and 1×10^{55} erg s^{-1}. The dependence of $L'_{\rm min}$ is estimated as follows. Equation (2·6), together with Eqs. (2·4) and (2·5), gives the approximate form $\psi_0 \sim (L'_{\rm min}/L'_*)^{-A}$. Then, Eq. (2·8) reads $\rho_0 \propto {\psi_0}^{-1} \propto (L'_{\rm min}/L'_*)^A$. Therefore, as shown in Table I, when $L'_{\rm min}$ becomes 10 times larger (smaller), ρ_0 becomes about 2 times smaller (larger). Finally, we find that ρ_0 changes by a factor of 2 when the parameters in the luminosity function are varied in ranges corresponding to 90% of the uncertainties on the observational results derived in Ref. 41).

Table I. The values of $\rho_0 = \rho(z=1)$ (in units of $\mathrm{Gpc}^{-3}\ \mathrm{yr}^{-1}$) for various luminosity ranges [see Eq. (2·2)].

		$L'_{\max}$ [a)]		
		1×10^{53}	1×10^{54}	1×10^{55}
$L'_{\min}$ [a)]	1×10^{48}	1.69	1.63	1.62
	1×10^{49}	0.86	0.84	0.83
	1×10^{50}	0.44	0.43	0.43

a) The maximum and minimum luminosities in units of erg s^{-1} [see Eq. (2·7)].

We obtain $\rho(0) \simeq 0.01\ \mathrm{Gpc}^{-3}\mathrm{yr}^{-1}$ and $\rho(1) \simeq 1.0\ \mathrm{Gpc}^{-3}\mathrm{yr}^{-1}$ in this paper. Let us compare these with previous results. From the results obtained in Ref. 9), in which the functional form of $\rho(z)$ is determined so as to reproduce both the observed peak flux and redshift distributions, the values $\rho(0) \simeq 0.04$–$0.4\ \mathrm{Gpc}^{-3}\mathrm{yr}^{-1}$ and $\rho(1) \simeq 0.2$–$3.8\ \mathrm{Gpc}^{-3}\mathrm{yr}^{-1}$ can be inferred. We thus find that our results are roughly consistent with those derived in Ref. 9). However, Schmidt[35] estimated the local GRB rate density to be $\rho(0) \sim 0.5\ \mathrm{Gpc}^{-3}\mathrm{yr}^{-1}$, which is more than one order of magnitude higher than our value. This difference may result from an insufficient amount of data and low resolution in the redshift range $0 < z < 1$. The form of $\rho(z)$ we employ might be steeper than the actual one. Therefore, because the function $\rho(z)$ is normalized at $z = 1$ in this paper, the local GRB rate that we derived at $z = 0$ might be smaller than the actual value.

2.2. *GRB formation rate corrected by the jet opening angle*

We consider the *true* rate of GRBs which actually occurred in the redshift range $z_1 < z < z_2$. For this purpose, it is necessary to consider the geometrical correction of the jet opening angle, θ_j. Although the jet structure is still unknown, we employ a uniform jet model. Taking into account the correction due to jet collimation, the cumulative GRB rate is calculated as

$$N(z_1,z_2) = \int_{z_1}^{z_2} dz\,\frac{1}{1+z}\frac{dV}{dz}\int_{L_{\min}(z)}^{L_{\max}(z)} dL\,\Phi(L,z) \times \int dL_j\,P(L_j,z)\,f_b(L,L_j)^{-1} \quad , \tag{2·10}$$

where L_j and f_b are the peak luminosity confined in the jet and the beaming factor, given by

$$f_b(L,L_j) = 1-\cos\theta_j(L,L_j) = \frac{L_j}{L}\ (<1) \quad , \tag{2·11}$$

respectively. The quantity L_j is assumed to be clustered in a narrow range around the standard value,[21] and its distribution is approximately log-normal:

$$P(L_j,z) = \frac{1}{\sqrt{2\pi}\sigma L_j}\exp\left[-\frac{1}{2\sigma^2}\left(\log L_j - \log\tilde{L_j}(z)\right)^2\right] \quad , \tag{2·12}$$

where $\log \tilde{L}_j(z)$ and σ are the mean and standard deviation of the luminosity distribution, respectively. In this paper, the evolution of the jet-corrected luminosity is assumed to take the simple form

$$\tilde{L}_j(z) = L_{j1} \left(\frac{1+z}{2} \right)^{\beta} \quad , \tag{2·13}$$

where β is the slope index of the jet-luminosity evolution. We discuss in §3 the validity of our assumed functional forms of $P(L_j, z)$ and $\tilde{L}_j$.

Substituting Eqs. (2·1), (2·11), (2·12), and (2·13) into Eq. (2·10), we obtain the cumulative GRB rate as

$$N(z_1, z_2) = \int_{z_1}^{z_2} dz \, \frac{1}{1+z} \frac{dV}{dz} \rho(z) \left\langle f_b^{-1} \right\rangle_z \ , \tag{2·14}$$

where

$$\begin{aligned} \left\langle f_b^{-1} \right\rangle_z &\equiv \frac{\int_{L_{\min}(z)}^{L_{\max}(z)} dL \, \Phi(L,z) \, L / \left\langle L_j \right\rangle_z}{\int_{L_{\min}(z)}^{L_{\max}(z)} dL \, \Phi(L,z)} \\ &= \frac{10^{\frac{1}{2}\sigma^2 \ln 10}}{L_{j1}} \left(\frac{1+z}{2} \right)^{\alpha-\beta} \int_{L'_{\min}}^{L'_{\max}} dL' \, \phi(L') \, L' \end{aligned} \tag{2·15}$$

is the luminosity weighted beaming factor, and

$$\begin{aligned} \left\langle L_j \right\rangle_z &\equiv \left[\int dL_j \, P(L_j, z) L_j^{-1} \right]^{-1} \\ &= \frac{L_{j1}}{10^{\frac{1}{2}\sigma^2 \ln 10}} \left(\frac{1+z}{2} \right)^{\beta} \end{aligned} \tag{2·16}$$

is the mean jet-luminosity.

We choose the value of $\left\langle L_j \right\rangle_{z=1} = L_{j1} / 10^{\frac{1}{2}\sigma^2 \ln 10}$ so that $\left\langle f_b^{-1} \right\rangle_z$ is 200 at $z = 1$. In this case, the mean jet opening half-angle, defined by $\left\langle \theta_j \right\rangle_z \equiv [\left\langle f_b^{-1} \right\rangle / 2]^{-1/2}$, is equal to the typical value of 0.1 rad at $z = 1$. Then we find

$$\begin{aligned} \left\langle L_j \right\rangle_{z=1} &\equiv \frac{L_{j1}}{10^{\frac{1}{2}\sigma^2 \ln 10}} \\ &= 2.5 \times 10^{49} \text{ erg s}^{-1} \left(\frac{\left\langle f_b^{-1} \right\rangle_{z=1}}{200} \right)^{-1} \end{aligned} \tag{2·17}$$

with the fiducial parameters ($L'_{\max} = 1 \times 10^{54}$ erg s^{-1} and $L'_{\min} = 1 \times 10^{49}$ erg s^{-1}). The value of $\left\langle L_j \right\rangle_{z=1}$ changes by only a factor of 3 when $L'_{\max}$ and $L'_{\min}$ vary between 1×10^{53} and 1×10^{55} erg s^{-1} and between 1×10^{48} and 1×10^{50} erg s^{-1}, respectively. Substituting Eq. (2·17) into Eq. (2·15), we derive

$$\left\langle f_b^{-1} \right\rangle_z = 200 \left(\frac{1+z}{2} \right)^{\alpha-\beta} \left(\frac{\left\langle f_b^{-1} \right\rangle_{z=1}}{200} \right) \quad , \tag{2·18}$$

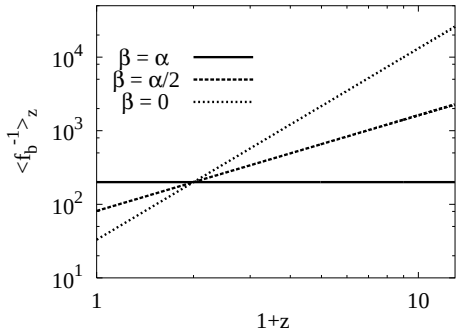

Fig. 1. Luminosity-weighted beaming factor $\left\langle f_b^{-1} \right\rangle$ as a function of the source redshift z. The solid, dashed, and dotted lines correspond to $\beta = \alpha$, $\alpha/2$, and 0, respectively. In the case $\beta = \alpha$ (solid line), the beaming factor is independent of z, with the value $\left\langle f_b^{-1} \right\rangle = 200$.

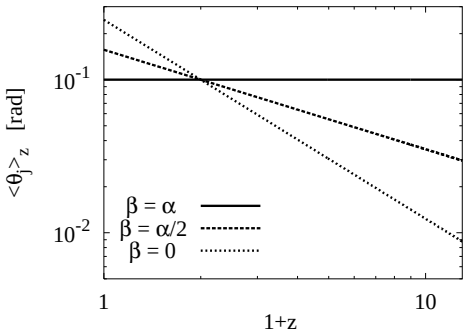

Fig. 2. Mean opening half-angle $\langle \theta_j \rangle$ as a function of the source redshift z. The solid, dashed, and dotted curves correspond to $\beta = \alpha$, $\alpha/2$, and 0, respectively. In the case $\beta = \alpha$ (solid line), the mean jet opening angle is independent of z, with the value $\langle \theta_j \rangle = 0.1$ rad.

and

$$\langle \theta_j \rangle_z = 0.1 \left(\frac{1+z}{2} \right)^{\gamma} \left(\frac{\left\langle f_b^{-1} \right\rangle_{z=1}}{200} \right)^{-1/2} , \qquad (2{\cdot}19)$$

where $\gamma = (\beta - \alpha)/2$.

Figures 1 and 2 display the luminosity-weighted beaming factor, $\left\langle f_b^{-1} \right\rangle_z$, and the mean opening half-angle, $\langle \theta_j \rangle_z$, as functions of z. The value of β is uncertain. As seen in Table II, we consider three cases: $\beta = \alpha$ (*no jet-opening angle evolution*), $\beta = \alpha/2$ (*intermediate*), and $\beta = 0$ (*no jet-luminosity evolution*). In the case $\beta = 0$, we find $\left\langle f_b^{-1} \right\rangle_z \sim 3 \times 10^4$ and $\langle \theta_j \rangle_z \sim 9 \times 10^{-3}$ for $z \sim 12$ in the fiducial case. The latter is about 10 times smaller than the typical value for $z \sim 1$. By contrast, when $\beta = \alpha = 2.6$, the beaming factor is independent of z, and we have $\left\langle f_b^{-1} \right\rangle = 200$. However, the mean jet-corrected luminosity $\tilde{L}_j$ increases with z [see Eq. (2·13)] and $\tilde{L}_j(12) \sim 1.3 \times 10^2 \tilde{L}_j(1)$, which is also unnatural. Hence, intermediate values of β, in the neighborhood of $\beta \sim \alpha/2$, for which both $\tilde{L}_j$ and $\left\langle f_b^{-1} \right\rangle$ depend on z, may be preferable.

Table II. Models.

β	Evolution
α	**Jet-luminosity evolution** (*no jet-opening angle evolution*)
$\alpha/2$	**Inter-mediate**
0	**Jet-opening angle evolution** (*no jet-luminosity evolution*)

Figure 3 plots the cumulative GRB rate $N(0, z)$ as a function of z, which is the GRB frequency at redshifts smaller than z. When we vary β from α to 0, $N(0, z_{\max})$ increases by approximately one order of magnitude, and the deviation becomes larger for higher redshift.

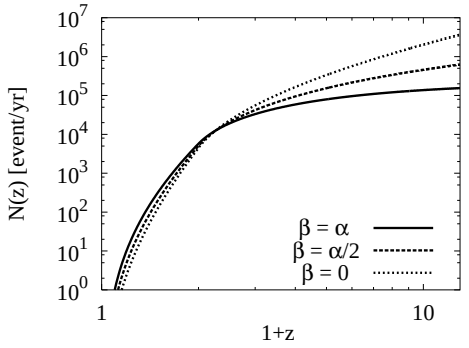

Fig. 3. The cumulative GRB rate $N(0,z)$ [see Eq. (2·14)]. The solid, dashed, and dotted curves correspond to $\beta=\alpha$, $\alpha/2$, and 0, respectively. These are frequencies of GRBs that actually occurred at redshifts from 0 to z.

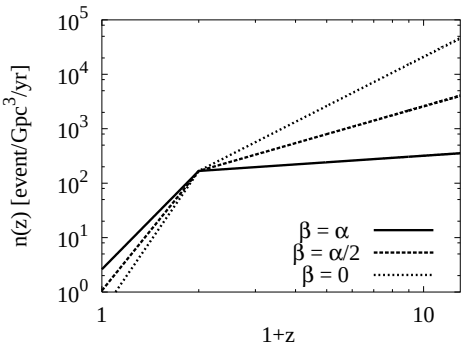

Fig. 4. The comoving GRB rate density $n(z)$. The solid, dashed, and dotted curves correspond to $\beta=\alpha$, $\alpha/2$, and 0, respectively. In the case $\beta=\alpha$, $n(z)$ is simply proportional to $\rho(z)$.

Finally, the *true* comoving GRB rate density is given by

$$n(z) = (1+z)\left(\frac{dV}{dz}\right)^{-1}\frac{d}{dz}N(0,z) = \rho(z)\left\langle {f_b}^{-1}\right\rangle_z \quad . \tag{2·20}$$

Figure 4 presents the results. In the case $\beta=\alpha$, the value of $\left\langle f_b^{-1}\right\rangle_z$ does not depend on z, and thus $n(z)$ is simply proportional to $\rho(z)$. It is also seen that when the jet opening angle evolution is considered ($\beta<\alpha$), the GRB rate at high redshift becomes much larger than that at low-z.

§3. Discussion

We have estimated the absolute GRB rate taking into account the effects of jet collimation. The normalization constant, ρ_0, was chosen so as to reproduce the BATSE detection rate of bright GRBs with observed fluxes larger than 2×10^{-7} erg cm^{-2}s^{-1}. In this paper, we specifically considered for the first time both the jet luminosity evolution and the jet opening angle evolution. Both evolution effects are important because when only one of them is taken into account, extreme results are obtained in the high redshift regime, say, $z>10$. When the mean jet opening angle does not depend on z ($\beta=\alpha$; *no jet-opening angle evolution*), the jet-corrected luminosity $\tilde{L}_j$ for high-redshift GRBs is much larger than the typical values for $z\sim1$ bursts. On the other hand, when $\tilde{L}_j$ is independent of z ($\beta=0$; *no jet-luminosity evolution*), the jet opening angle for high-z bursts should be much smaller than that for low-z GRBs. Therefore, the intermediate case ($\beta\sim\alpha/2$), in which both $\tilde{L}_j$ and the jet opening angle varies with z, is most preferable. It is also found that for any value of β, the true GRB rate $n(z)$ does not decrease for high-z as long as $z<12$, and might not be simply proportional to the cosmic star

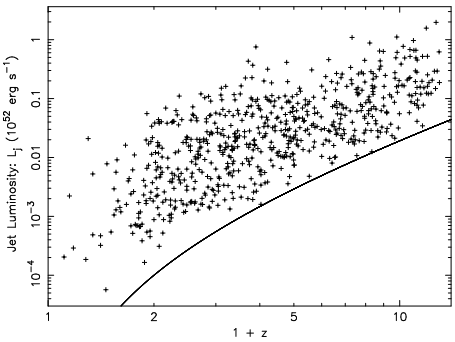

Fig. 5. Distribution of the jet-corrected luminosity $L_j = f_b L$ (with $f_b = 1 - \cos\theta_j$, where θ_j is the jet opening half angle) as a function of the redshift. The redshift is estimated using the spectral peak energy-peak luminosity relation (the Yonetoku relation),[41] and θ_j is estimated[42] using the Yonetoku relation and the spectral peak energy-jet corrected energy relation (the Ghirlanda relation).[13] The solid curve represents the truncation of the upper bound of L_j that is caused by the flux limit $F_{\rm lim} = 1 \times 10^{-6}$ erg cm^{-2}s^{-1}.

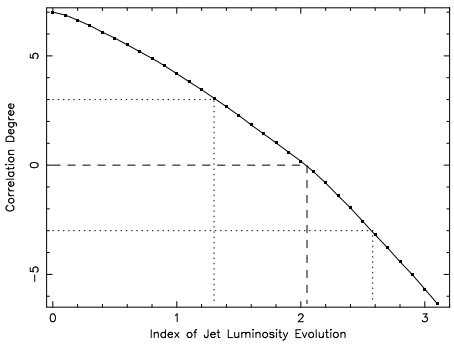

Fig. 6. The best index of the jet luminosity evolution measured using the τ-statistical method. When we assume L_j evolution as a function of $(1+z)^\beta$, $\beta = 2.05$ is the best value, at which the data correction degree becomes zero. We also plot upper and lower bounds of the index corresponding to 3σ from the best value. These bounds are given by $\beta = 2.58$ and $\beta = 1.30$. The value $\beta = 0$ lies approximately 8σ from the best value, and hence we reject this case in which L_j-evolution does not exist.

formation rate. These facts might imply that the metalicity affects the properties of the GRB progenitor. For example, in the high-redshift epoch, because of the low metalicity, the opacity of a star was small and the stellar envelope may not be blown off completely. Then, it might be difficult for the GRB jets to break out of the stellar surface, resulting in small opening angles.

Recently, the existence of opening angle evolution of the form $\propto (1+z)^\gamma$ with $\gamma = -0.45^{+0.20}_{-0.18}$ was suggested in Ref. 42). Combining this with the result $\alpha = 2.6^{+0.15}_{-0.20}$ derived in Ref. 41), we find $\beta = \alpha + 2\gamma = 1.70^{+0.43}_{-0.41}$, and thus $\beta \simeq \alpha/2$. The jet luminosity evolution is seen more clearly in Fig. 5. Here we use the data set analyzed in Ref. 42). Also, the redshifts and opening angles are estimated in the same manner as in Ref. 42). In this way, we can obtain the jet-collected luminosity L_j as a function of $(1 + z)$. Using the generalized tau statistical method,[32),23),22),41),42)] we obtain $\beta = 2.05^{+0.53}_{-0.75}$ (see Fig. 6), which is consistent with the value $\beta = 1.70^{+0.43}_{-0.41}$, which is predicted using the combination of the luminosity evolution and the jet opening angle evolution. Furthermore, Fig. 5 shows that L_j is clustered in a narrow range around the mean value for each z and that the distribution of L_j for a given bin of $1 + z$ roughly takes the form of a log-normal with a logarithmic mean σ of approximately 0.6. [When we adopt $\sigma \sim 0.6$ and $\left\langle f_b^{-1} \right\rangle_{z=1} = 200$, we find $L_{j1} \sim 3 \times 10^{49}$ erg s^{-1} from Eq. (2·17).] We believe that σ is independent of z, as assumed in this paper, but, the lack of statistics prevents us from carrying out a more detailed study of this point. Of course, our method to estimate L_j contains many uncertainties, and hence more direct estimations of z and θ_j are necessary. If the *Swift* satellite collects data

from many events with spectroscopically measured redshifts and jet opening angles determined from the wavelength-independent achromatic break in the afterglow light curves, our understanding of evolution effects will be tested.

Using the local GRB rate, the event rate per galaxy can be estimated as

$$r_{\rm GRB} = n(z)/n_{\rm gal} \simeq 1 \times 10^{-5}\ {\rm yr}^{-1}\ {\rm galaxy}^{-1} \left(\frac{n(z)}{10^2\ {\rm yr}^{-1}\ {\rm Gpc}^{-3}}\right)\left(\frac{n_{\rm gal}}{10^7\ {\rm Gpc}^{-3}}\right)^{-1} , \quad (3\cdot1)$$

where $n_{\rm gal}$ is the total number density of spiral and elliptical galaxies, which is typically $\sim 1 \times 10^7$ Gpc^{-3}.[26] In the case $\beta = \alpha/2$, we obtain $r_{\rm GRB} = 2 \times 10^{-5}$ yr^{-1} galaxy^{-1} for $z = 1$ and $r_{\rm GRB} = 1 \times 10^{-7}$ yr^{-1} galaxy^{-1} for $z = 0$. Sokolov[36] independently estimated the result $r_{\rm GRB} \sim 5 \times 10^{-8} \left\langle {f_b}^{-1} \right\rangle$ yr^{-1} galaxy^{-1}, which is roughly consistent with our result. Our values are comparable to the local rate of core-collapse (energetic Type Ib/Ic) SNe, $\sim 10^{-6}$–10^{-5}yr^{-1} galaxy^{-1},[33] although the rate for type Ib/Ic SN at high redshift is not known. Even if collimated ultra-relativistic outflow and relativistic beaming effect prevent us from observing prompt GRB emissions far from the jet axis, the emissions from associated energetic core-collapse SNe are nearly isotropic. Hence, the expected SN rate can be estimated as $N(0, z_{\rm SN})$. The *Supernova/Acceleration Probe*[*] will detect SNe with redshifts of up to $z_{\rm SN} \sim 1.7$, and thus we expect $N(0, z_{\rm SN} = 1.7) \sim 3 \times 10^4$ events yr^{-1}.

Acknowledgments

This work was supported in part by Grants-in-Aid for Scientific Research of the Japanese Ministry of Education, Culture, Sports, Science and Technology [No. 09245 (RY) and 15740149 (DY)]. TM is supported by the Junior Research Associate Program at RIKEN (The Institute of Physical and Chemical Research), Japan.

References

1) L. Amati et al., Astron. Astrophys. **390** (2002), 81.
2) J. L. Atteia, Astron. Astrophys. **407** (2003), L1.
3) R. Barkana and A. Loeb, Astrophys. J. **601** (2004), 64.
4) J. S. Bloom, D. A. Frail and S. R. Kulkarni, Astrophys. J. **594** (2003), 674.
5) D. Caditz and V. Petrosian, Astrophys. J. **357** (1990), 326.
6) B. Ciardi and A. Loeb, Astrophys. J. **540** (2000), 687.
7) M. Della Valle et al., Astron. Astrophys. **406** (2003), L33.
8) E. E. Fenimore and E. Ramirez-Ruiz, astro-ph/0004176
9) C. Firmani, V. Avila-Reese, G. Ghisellini and A. V. Tutukov, Astrophys. J. **611** (2004), 1033
10) D. A. Frail et al., Astrophys. J. **562** (2001), L55.
11) S. R. Furlanetto and A. Loeb, Astrophys. J. **579** (2002), 1.
12) T. J. Galama et al., Nature **395** (1998), 670.
13) G. Ghirlanda, G. Ghisellini and D. Lazzati, Astrophys. J. **616** (2004), 331.
14) D. Guetta, T. Piran and E. Waxman, Astrophys. J. **619** (2005), 412.
15) D. Guetta, J. Granot, M. Begelman Astrophys. J. **622** (2005), 482.
16) J. Hjorth et al., Nature **423** (2003), 847.
17) S. Inoue, Mon. Not. R. Astron. Soc. **348** (2004), 999.

[*] `http://snap.lbl.gov/`

18) A. K. Inoue, R. Yamazaki and T. Nakamura, Astrophys. J. **601** (2004), 644.
19) K. Ioka, Astrophys. J. **598** (2003), L79.
20) D. Q. Lamb and D. E. Reichart, Astrophys. J. **536** (2000), 1.
21) D. Q. Lamb, T. Q. Donaghy and C. Graziani, Astrophys. J. **620** (2005), 355.
22) N. M. Lloyd-Ronning, C. L. Fryer and E. Ramirez-Ruiz, Astrophys. J. **574** (2002), 554.
23) A. Maloney and V. Petrosian, Astrophys. J. **518** (1999), 32.
24) A. Maloney and V. Petrosian, Astrophys. J. **524** (1999), 262.
25) P. Mészáros Annu. Rev. Astron. Astrophys. **40** (2002), 137.
26) S. L. W. McMillan and S. F. Portegies Zwart, AIP Conf. **575** (2001), 119.
27) T. Murakami, D. Yonetoku, H. Izawa and K. Ioka, Publ. Astron. Soc. Jpn. **55** (2003), L65.
28) T. Murakami, D. Yonetoku, M. Umemura, T. Matsubayashi and R. Yamazaki, Astrophys. J. **625** (2005), L13.
29) J. P. Norris, G. F. Marani and J. T. Bonnell, Astrophys. J. **534** (2000), 248.
30) W. S. Paciesas et al., Astrophys. J. Suppl. **122** (1999), 465.
31) R. Perna, R. Sari and D. Frail, Astrophys. J. **594** (2003), 379.
32) V. Petrosian, Astrophys. J. **402** (1993), L33.
33) Ph. Podsiadlowski, P. A. Mazzali, K. Nomoto, K., D. Lazzati and E. Cappellaro, Astrophys. J. **607** (2004), L17.
34) M. Schmidt, Astrophys. J. **523** (1999), L117.
35) M. Schmidt, Astrophys. J. **552** (2001), 36.
36) V. V. Sokolov, in proc. Second Rome Workshop: Gamma-Ray Bursts in the Afterglow Era, ed. E. Costa, F. Frontera and J. Hjorth (Berlin: Springer), 136 (2001) (astro-ph/0102492)
37) D. Spergel et al., Astrophys. J. Suppl. **148** (2003), 175.
38) K. Z. Stanek et al., Astrophys. J. **591** (2003), L71.
39) T. Totani, Astrophys. J. **486** (1997), L71.
40) D. M. Wei, Mon. Not. R. Astron. Soc. **345** (2003), 743.
41) D. Yonetoku, T. Murakami, T. Nakamura, R. Yamazaki, A. K. Inoue and K. Ioka, Astrophys. J. **609** (2004), 935.
42) D. Yonetoku, R. Yamazaki, T. Nakamura and T. Murakami, Mon. Not. R. Astron. Soc. **362** (2005), 1114.
43) B. Zhang and P. Mészáros, Int. J. Mod. Phys. **A19** (2003), 2385.